



Research Article

Strategic design and optimization of ultra-high-frequency regenerators for miniature pulse tube cryocoolers: A roadmap to achieve high efficiency and compact

Chetan O. YADAV^{1,*}, P. V. RAMANA¹

¹Department of Mechanical Engineering, Sardar Vallabhbhai Patel Institute of Technology, Gujarat, 388306, India

ARTICLE INFO

Article history

Received: 27 April 2024

Revised: 19 December 2024

Accepted: 19 December 2024

Keywords:

Miniature Pulse Tube
Cryocooler; REGEN3.3;
Regenerator; Ultra-High
Frequency

ABSTRACT

Infrared sensors on small satellites require a miniature pulse tube cryocooler to operate efficiently at ultra-high frequencies. This study focuses on optimizing the regenerator of a miniature pulse tube cryocooler, which is crucial for enhancing performance in terms of low vibration, improving reliability, and increasing the system's lifespan. Using the software tool REGEN 3.3, we conducted numerical simulations to analyze the geometrical and operating parameters that impact the performance of the ultra-high frequency regenerator. A comprehensive investigation was performed across a wide range of ultra-high frequencies (100 to 200 Hz), charge pressures (3.5–7.0 MPa), and pressure ratios (1.15–1.3), while considering operating temperatures from 300 K to 80 K and cooling power of 1 W. The optimized regenerator dimensions of 4 mm diameter and 25 mm length at 100 Hz achieve a coefficient of performance of 0.0819, while at 200 Hz, dimensions of 4 mm diameter and 20 mm length produce a coefficient of performance of 0.07491, demonstrating frequency-dependent performance variation. The Key results show that variations in regenerator length by up to 20% (from 25 mm to 20 mm) result in only a 5.093% decrease in coefficient of performance, while a 30% increase (from 25 mm to 30 mm) leads to a 14.91% reduction. The findings indicate that operating frequency minimally influences the optimal diameter; however, the optimum regenerator length decreases with frequency. An increase in frequency from 100 Hz to 200 Hz results in a 20% reduction in regenerator length and an 8.51% decrease in COP. Charge pressure has a limited effect on optimal dimensions, whereas higher cold-end pressure ratios significantly reduce the overall dimensions of the regenerator. An increase in charge pressure reduces pressure drop loss by up to 73% with no significant effect on regenerator losses, while the variations in the pressure ratio have no significant impact on pressure and regenerator losses. The novelty of this work lies in its systematic numerical optimization of an ultra-high frequency regenerator for miniature pulse tube cryocoolers, providing insights that extend beyond previous literature by demonstrating the importance of broad tolerances in design parameters and the significant impact of geometry and operating parameters on performance. This study outlines a roadmap of the ultra-high-frequency regenerator in miniature pulse tube cryocoolers, facilitating efficient operation and miniaturization, thereby enhancing the capabilities of satellite systems.

Cite this article as: Yadav CO, Ramana PV. Strategic design and optimization of ultra-high-frequency regenerators for miniature pulse tube cryocoolers: A roadmap to achieve high efficiency and compact. J Ther Eng 2025;11(3):824–844.

*Corresponding author.

*E-mail address: coyadav@gmail.com

This paper was recommended for publication in revised form by Editor-in-Chief Ahmet Selim Dalkılıç



INTRODUCTION

The development of miniature electronic technologies in space applications, like remote sensing, data transmission, infrared imaging, etc. requires miniature cryocoolers for their thermal management at temperatures ranging from 60K - 80 K with small payloads up to 1 W. Stirling Cryocoolers have effectively cooled infrared sensors for years, leading to advancements that limit the use of pulse tube cryocoolers (PTC) [1]. However, the mechanical displacer at the cold end of the Stirling cryocooler produces vibration and thus reduces longevity. In the past few years, there has been considerable progress in the design of PTCs. The combination of pulse tube, inertance tube, and surge volume in PTC design allows for the removal of mechanical components at the cold end, as shown in Figure 1.

By removing this mechanical element, the PTC experiences reduced vibration, enhancing reliability and extending operational lifespan. These characteristics are particularly advantageous for space applications, where stability, durability, and longevity are paramount. The regenerator is typically framed of different structures and geometries in a thin-walled metallic tube. The hot and cold gases flow periodically within the regenerator matrices. The matrix stores the heat released by the hot gas during the hot blow period and rejects the same stored heat to the cold gas during the cold blow period, thus completing the thermal cycle. One of the most challenging tasks in the PTC is scaling down compared to the Stirling cryocooler while maintaining the same high efficiency. Miniaturization of the PTC alters the governing parametric quantities that apply to conventional PTCs. One of the limiting factors for the miniaturization of the PTC is the reduction of the working gas volume, and the effectual solution to compensate is to enhance the power density by increasing the operating frequency and filling higher charge pressure[2, 3]. Miniature Pulse Tube Cryocoolers (MPTC) operating at ultra-high frequencies exceeding 100 Hz are designed to enable compact dimensions while maintaining high efficiency and performance. The system’s regenerator significantly affects

the miniature cryocooler’s overall thermal performance at these frequencies.

Several researchers have attempted the miniaturization of the pulse tube cryocoolers. Vanapalli et al. [4] optimized the regenerator of their MPTC using REGEN 3.2 software tools, resulting in dimensions of 9.02 mm inner diameter and 30 mm length. They attributed the system’s high efficiency to using a denser wire mesh screen (SS 635 #) within the regenerator. However, the system’s ability to achieve the theoretical high frequency was hindered by being driven by a relatively larger commercially available compressor. Radebaugh et al. [5] designed the regenerator for their MPTC using REGEN 3.2 and SAGE 4.0 software tools for a frequency of 150 Hz, with an operating charge pressure of 5.0 MPa and a pressure ratio of 1.3, aiming for a cooling power of 1W@80K. However, in experimental trials, they achieved only a pressure ratio of 1.13 instead of the designed 1.30. Despite this discrepancy, the system reached a no-load temperature of 97.5 K within approximately 100 seconds. The researchers concluded that the regenerator design would likely perform even better at increased frequencies and pressure ratios. Wang et al. [6] conducted an analytical and experimental investigation on an MPTC operating at frequencies of 100 Hz and 280 Hz. They observed that as the frequency increased from 100 Hz to 280 Hz, the performance of the PTC deteriorated, resulting in a reduction in cooling power from 2.8 W@77 K to 1W@ 80 K. This degradation was attributed to the unsuitability of the regenerator matrix material. Mohan and Atray [7] designed and developed an MPTC with a total pulse tube and regenerator volume of 1.72 cc, operating at a very high frequency of 148 Hz. Ouyang et al. [8] developed an MPTC operating at a frequency of 118 Hz with an overall cryocooler weight of 930 grams with a cold finger external diameter of 10 mm. The cooling power achieved by the system is 1.24 W @ 80K with an input power of 35 W. A 2-D regenerator model is developed to optimize hybrid stainless steel wire mesh structures for Stirling-type PTC. This study examines the characteristics of heat transfer and pressure drop, supported by experimental data to confirm the

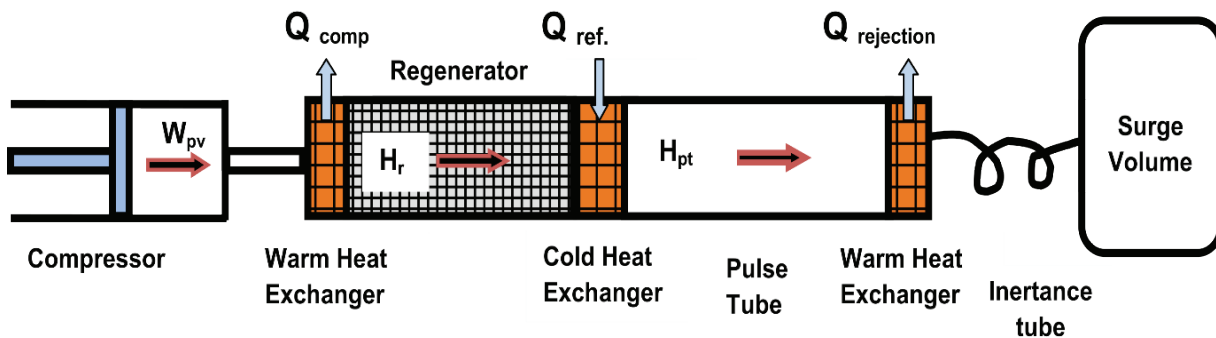


Figure 1. Pulse tube cryocooler.

theoretical outcomes [9]. Shaoshuai Liu et al. [10] examine how operating parameters like charge pressure and frequency affect the cooling efficiency of PTCs. Their study shows that optimizing these frequency parameters of 51 and 52 Hz and average pressures between 2.5 MPa and 3.5 MPa can greatly minimize regenerator losses and optimize phase angles, leading to increased cooling efficiency. They report achieving a cooling power of 10W at 80 K with a (COP) coefficient of performance of 16.0% and compressor efficiencies of up to 88%. Garg et al. [11] investigated the effect of porous regenerators on miniature Stirling cryocooler efficiency, finding that lower porosity increases power consumption due to higher pressure drops, while higher porosity reduces power input but impairs thermal performance. Zhao et al. [12] developed a CFD model to study the impact of frequency and pulse tube length on a micro coaxial Stirling-type PTC, highlighting the need for further exploration of regenerator geometries to optimize performance and compactness. Malwe et al. [13] investigated the performance and exergy of a PTC at 80 K, testing charge pressures of 12, 14, and 16 bar. Results indicated that the refrigerating effect increased with higher charge pressure. For optimal performance at 70 K and a 15 W cooling load, 16 bar was identified as optimal, with a pulse tube diameter of 9.6 mm and length of 128.5 mm. Further studies on higher charge pressures and additional parameters are needed for miniaturization. Abraham and Kuzhiveli [14] investigated the effect of stainless-steel mesh characteristics on PTC performance. They found that using multi-mesh configurations improved efficiency and heat transfer. Additionally, incorporating multi-mesh regenerators with an inertance tube and bounce space as a phase shifter increases the COP. This research highlights the critical importance of mesh configuration in optimizing PTC performance. Guo and Zhu [15] highlighted the crucial role of the regenerator in their study of a micro-PTC with a displacer phase shifter. They determined that adjusting the regenerator's design is essential for maintaining efficient cooling power across different pulse tube diameters, showcasing its essential contribution to improving cryocooler performance. Guo and Zhu [16] conducted a numerical study examining the regenerative impact of heat exchangers in PTCs. Their findings indicate that the regenerative effect diminishes expansion work, as measured by enthalpy flow, thereby decreasing system performance, particularly at higher pressure ratios. Feng et al. [17] developed a micro pulse tube cryocooler featuring a regenerator with a diameter of 10 mm and a length of 42 mm. This system, weighing 598 grams, achieves a cooling power of 1.2 W at 80 K, utilizing a compressor input power of 45 W within a remarkably short duration of just 3 minutes. Zhao et al. [18] developed a CFD model for a coaxial Stirling-type PTC operating at 125 Hz, analyzing how operating frequency affects fluid dynamics and thermal transfer in the regenerator. Li et al. [19] discuss a micro coaxial type PTC optimized for infrared detection at an optimal frequency of 175 Hz. Their study emphasizes specific

geometrical configurations, such as regenerator length, larger dimensions, and matrix type, while considering diameter. However, their focus on charge pressure limits a comprehensive understanding of the system's overall performance. This highlights the need for a more systematic approach to explore the interactions among various design elements, potentially enhancing insights into the cryocooler's efficiency and effectiveness. Min et al. [20] examined a specific regenerator design incorporating a middle heat exchanger through numerical and experimental approaches but did not investigate a wider range of geometrical configurations. The use of fixed operational parameters limits the research and does not provide a systematic analysis of how different regenerator lengths and configurations affect overall efficiency. Wang et al. [21] developed a coaxial-type single-stage PTC that operates at a frequency of 102 Hz, which may not be suitable for all applications. While this design is lighter than traditional models, its weight of 4.4 kg poses challenges for ultra-lightweight in space applications. Zhiet al. [22] conducted an experimental study on an MPTC, offering valuable insights into its refrigeration performance. However, the investigation primarily focuses on the cryocooler's performance at a fixed charge pressure of 4 MPa, with input electric powers of 30 W and 68 W, and a frequency of 115 Hz. The highest cooling capacity achieved was 1.73 W at a temperature of 77 K. This limited focus restricts the exploration of how variations in other geometrical and operational parameters impact overall system performance.

Several studies have investigated regenerators and their influence on cryocooler performance with REGEN. REGEN 3.3 is a software tool used for designing and optimizing to achieve the desired heat lift and cold end temperature. Pfothenauer et al. [23] conducted optimization of a regenerator operating at the frequency (30 Hz to 60 Hz), warm end temperature of 300 K, cold end temperatures (60 K, 80 K), cooling power (100 W to 900 W), area (0.015 to 0.04 m²) and length (0.04 to 0.06 m) using software tool REGEN 3.2. However, their results are restricted to a fixed average pressure (2.0 MPa) and pressure ratio (1.2). Radebaugh et al. [24] investigated the performance of rare-earth materials in regenerators, analyzing porosities from 0.1 to 0.38 at 30 Hz and pressures of 0.3 MPa to 1.5 MPa using He-3 and He-4. They compared parallel holes and packed spherical ball structures, focusing on pressure loss and COP at 4K. This study highlights the importance of porosity and structural design in optimizing regenerator performance. Wang et al. [25] performed a comparative analysis using REGEN 3.2 to assess the performance of various regenerator filler materials, including steel wire screens (500 #), lead screens (500 #), and lead spheres at a high frequency of 40 Hz and a temperature of 35 K. They found that lead spheres, which have a greater volumetric specific heat capacity, exhibited the poorest performance of the three materials due to challenges related to heat transfer depth and pressure drop. In contrast, the SS 500 # wire

screen satisfied the design requirements for the matrix. Thota et al. [26] designed the PTC aimed for operation at a frequency of 100Hz for the payload of 1 W @ 80 K. They employed REGEN 3.3 and SAGE software for performance analysis at both component and system levels. Pfothner et al. [27] indicated that the performance of a cryocooler regenerator can be broadly optimized, with the potential for higher COP using denser SS 400# mesh and charge pressures above 2 MPa. Srinivasan et al.'s [28] comparison of ANSYS and REGEN for regenerator pressure drop yielded consistent results, confirming REGEN's reliability for the Stirling Cryocooler regenerator design. REGEN's precise prediction of pressure drop, validated across different inlet pressures, supports its effectiveness for cryocooler regenerator analysis and design. Srinivasan et al. [29] designed and developed a prototype regenerator using the Direct Metal Laser Sintering technique for a cryocooler. Yadav and Ramana [30] investigated the influence of a regenerator metal matrix on the operation of an MPTC operating at ultra-high frequencies. Desai et al. [31] conducted numerical studies on layered regenerator configurations in PTCs, focusing on low frequencies. Their findings demonstrated that a hybrid configuration outperformed traditional uniform regenerator matrix materials, highlighting its improved effectiveness. Chen et al. [32] introduce a novel approach using a 1D-CNN to predict regenerator performance in cryogenic refrigerators, streamlining calculations and achieving high accuracy in power, pressure ratio, and COP prediction. This method improves efficiency and promises to transform cryogenic refrigerator design with agile and precise optimization capabilities.

The literature emphasizes the need to optimize regenerators to enhance the performance of PTCs, primarily focusing on low frequencies. Numerous research studies have investigated the performance of regenerators and their impact on cooling performance, with results reported using tools such as REGEN and computational fluid dynamics (CFD). While there have been some improvements using CFD and experimental analysis of MPTCs, there is still a lack of understanding regarding geometrical and operating characteristics at ultra-high frequencies. The research gaps include the limited exploration of cryocooler performance at frequencies above 100 Hz, as most existing studies concentrate on lower frequencies. Additionally, the scarcity of resistance coefficient values based on experimental pressure drop data for ultra-high frequencies hinders the validation of CFD simulations, thus limiting their reliability for parametric studies. In contrast, REGEN software proves valuable for modeling the complex thermodynamic cycles of regenerative systems, such as pulse tubes and Stirling cryocoolers. Unlike CFD, REGEN does not directly simulate compression and expansion but uses boundary conditions at the regenerator's inlet and outlet to account for these effects. This approach allows REGEN to effectively capture dynamic processes, providing insights into cycle efficiency and cooling capacities while also requiring

less computational time and not relying on experimental hydrodynamic data, making it an efficient tool for predicting regenerator performance and advancing miniaturization efforts with an improved COP. The present work aims to address existing gaps by investigating the underexplored challenges of ultra-high frequency operation in MPTCs. The novelty of this work lies in its focus on its systematic numerical optimization of ultra-high frequency regenerators for MPTCs. This area has been underexplored in previous research. By exploring this gap, the study provides new insights and optimization strategies, offering valuable guidelines for designing more efficient and compact systems. This investigation employs state-of-the-art steel screens (SS 635#) as the regenerator matrix structure for an MPTC, focusing on systematically analyzing various operating parameters. These parameters encompass ultra-high frequencies ranging from 100 Hz to 200 Hz, charge pressures from 3.5 MPa to 7.0 MPa, and pressure ratios varying from 1.15 to 1.3. The primary focus is on evaluating their collective influence on the cooling performance of the cryocooler. Additionally, this study aims to develop a roadmap for an ultra-high frequency regenerator for the MPTC.

NUMERICAL METHODOLOGY

The REGEN 3.3 [33] is an industry-standard one-dimensional numerical software developed by the National Institute of Standards & Technology (NIST) for designing and optimizing cryocooler regenerators. Figure 2 and Figure 3 depict the main screen and input screens of REGEN 3.3, which accept various geometries and operating input parameters.

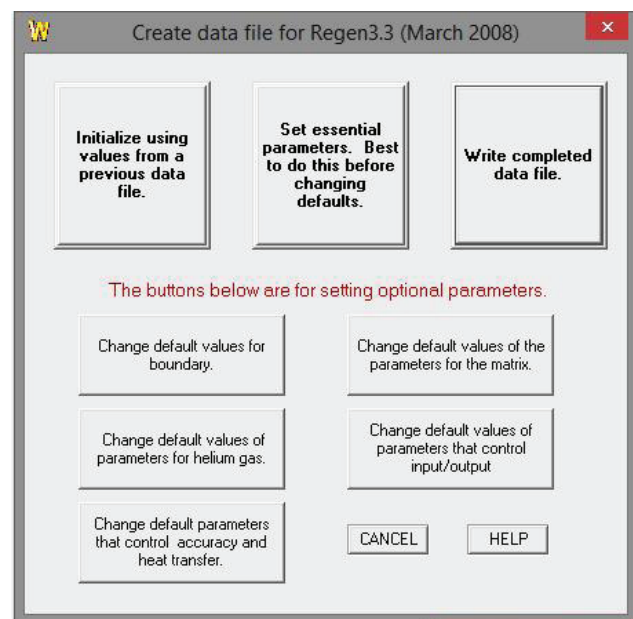


Figure 2. Main screen of REGEN 3.3 software.

Figure 3. Input screen of REGEN 3.3 software.

REGEN 3.3 software tools solve temperature-dependent thermal properties and provide good accuracy and stability making it the first choice for regenerator optimization by academicians and industries. REGEN 3.3 accommodates various input variables that users can freely define. These variables cover many parameters related to the regenerative cryocooler system, including temperature-dependent thermal properties, heat transfer correlations, fluid properties, geometrical and operational parameters, and others. It can efficiently process large amounts of data and perform numerical calculations to accurately model system behavior under various operating conditions. REGEN 3.3 provides comprehensive data output, including key performance indicators such as COP, pressure drop, heat transfer rates, temperature profiles, and other relevant parameters. This extensive output allows users to thoroughly analyze simulation results in detail and make well-informed decisions regarding system optimization. The comparison between results of REGEN 3.3 and Sage (used for system-level simulation software tool) are compared in terms of different parameters viz. hot end pressure ratio, phase angle, cooling power to PV input power over a range of temperature from 50 K to 150 K. The study concluded that there was excellent agreement between the simulation results obtained from REGEN and Sage. This finding provides high confidence in the thermodynamic modeling for cryocooler regenerators, indicating the reliability and accuracy of both software tools for such applications [34]. The results obtained from REGEN 3.2 software on high-frequency PTC are also validated with the experimentation [35].

The mass, momentum, and energy equations for conservation are solved by REGEN 3.3. The effect of the porous media in the mathematical model is considered by

incorporating the friction factors added to the momentum and energy equations. REGEN 3.3 is a full implicit model that solves non-linear equations for pressure, temperature, and mass flux at the grid points by Newton iteration simultaneously.

REGEN 3.3 [33] numerical model solves the following conservation equations for the fluid flow:

Mass Conservation Equation

$$\frac{\partial \rho}{\partial t} + \frac{\partial(\rho v)}{\partial x} = 0 \quad (1)$$

Momentum Equation

$$\frac{\partial \rho v}{\partial t} + \frac{\partial(\rho v^2 + p)}{\partial x} - f(\rho, T, v) = 0 \quad (2)$$

Where $f(\rho, T, v)$ is the friction term

$$\frac{\partial \phi A E}{\partial t} + \frac{\partial(\phi A(E + p)v)}{\partial x} - \frac{\partial(\phi A k_g)}{\partial x} - \phi A q(p, T, T_m, v) = 0 \quad (3)$$

$$\frac{\partial D}{\partial t} + \phi A q(p, T, T_m, v) - \frac{(1 - \phi) A k_m \frac{\partial T_m}{\partial x}}{\partial x} = 0 \quad (4)$$

Where the matrix material thermal term $D(x, T)$ is defined by

$$D(x, T) = \int_{T_{min}}^T (1 - \phi) A c_m(x, T) dT \quad (5)$$

The thermal term has the form

$$q(p, T, T_m, v) = 4H(p, T, v)(T_m - T)/D_h \quad (6)$$

Where $H(p, v)$ is the heat transfer coefficient

The determination of the COP involves normalizing the net refrigeration power concerning the PV work occurring at the hot end.

$$COP = \frac{NTCAD}{PVWKOT} \quad (7)$$

NTCAD represents the net cooling power of the regenerator, while PVWKOT denotes the PV work at the hot end of the regenerator.

The NTCAD is determined by calculating the PV work term at the cold end of the regenerator (PVWK1).

This is calculated from integral,

$$PVWK1 = \int_{t-\tau}^t \frac{\phi A v(L, t) p_a(L, t)}{\rho_c \tau} dt \quad (8)$$

Here, $v(L, t)$ and $\rho(L, t)$ represent the instantaneous velocity and density of the gas at the cold end of the regenerator, respectively. $p_d(t)$ denotes the instantaneous dynamic

pressure, while ρ_c indicates the gas density at the cold end temperature T_c

The NTCAD is found by

$$NTCAD = GRCAD - RGLOSS - HTFLUX - TUBECD \quad (9)$$

Where GRCAD is the gross cooling power for losses in the expansion space and is given by

$$GRCAD = (PVWK1-PRLOSS)*COOLING_MULT \quad (10)$$

PRLOSS (W) serves as the correction term utilized to assess the influence of pressurization on the enthalpy flux of the gas and obtained by

$$\max \int_{t-\tau}^t \frac{\phi A \rho(0,t) v(0,t) h(p(t), T_o)}{\tau} dt, \quad (11)$$

$$\int_{t-\tau}^t \frac{\phi A \rho(L,t) v(L,t) h(p(t), T_1)}{\tau} dt,$$

and COOLING_MULT is the factor used to estimate a reduced cooling power produced by a non-isothermal expansion process.

RGLOSS is the loss due to the regenerator’s ineffectiveness and it is given by

$$RGLOSS = ENTFLX - PRLOSS \quad (12)$$

ENTFLX denotes the integral average of the enthalpy flux at the cold side of the regenerator throughout one cycle and is given by

$$ENTFLX \int_{t-\tau}^t \frac{\phi A \rho(L,t) v(L,t) h(p(t), T(L,t))}{\tau} dt, \quad (13)$$

HTFLUX represents the heat transfer resulting from thermal conduction at the cold end of the regenerator.

While TUBECD refers to the thermal conduction occurring through the tube that housed the regenerator matrix. The tube material is assumed to be stainless steel, exhibiting a steady-state temperature profile. Thermal

exchange between the tube and the matrix is disregarded in the analysis. To calculate TUBECD the following formula is employed,

$$TUBECD = \frac{\sqrt{4\pi Ah}}{L} \int_{T_c}^{T_H} \sigma(T) dT \quad (14)$$

Where $\sigma(T)$ is the thermal conductivity of Stainless Steel.

The regenerator is constructed using a porous material with lower thermal, needing a correction factor for porosity in REGEN software.

Calculating the hot end PV work of the regenerator follows a methodology similar to equation 8 but with velocity and density evaluated at the hot end ($x=0$). To determine the pressure at the hot end, the pressure drop is added to the pressure at the cold end for a comprehensive analysis. The pressure drop is calculated through the integration of the pressure gradient.

Boundary Conditions and Solution Procedure

REGEN 3.3 is component-level design software, and thus it incorporates other components of the system, such as the compressor, pulse tube, and phase shift mechanisms modeled indirectly with the appropriate boundary conditions at both ends of the regenerator. REGEN 3.3 models presume sinusoidal mass flux at both ends (inlet and outlet) of the regenerator as an appropriate boundary condition. The regenerator numerical model is depicted in Figure 4.

The phase angle between the pressure and mass flow plays a crucial role in the performance of the regenerator, which in turn affects the overall efficiency of the cryocooler. Therefore, the mass flow rate (s) and phase angle at the cold end (s) for a fixed cold end PV work value were calculated. Input parameters needed in REGEN 3.3 are gas inflow at the hot end and cold end temperature, pressure ratio, average pressure, operating frequency, flow amplitude, hydraulic diameter, cold end phase angle, and the geometrical parameters of the matrices i.e. matrix material, length of regenerator, porosity, cross-sectional area. Input

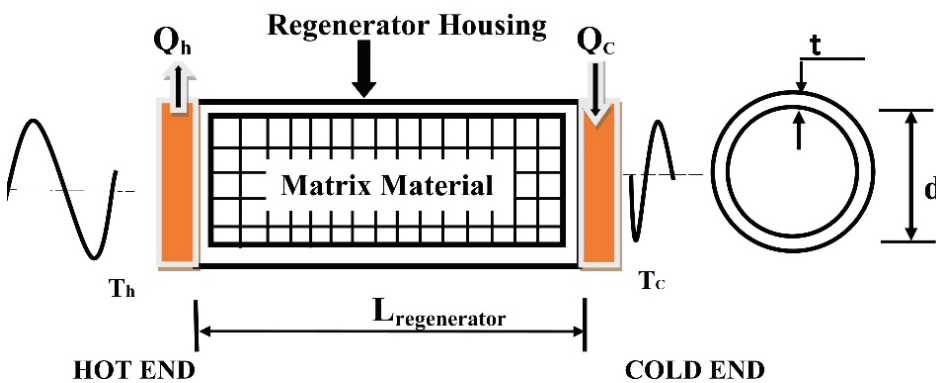


Figure 4. Model of regenerator in REGEN 3.3.

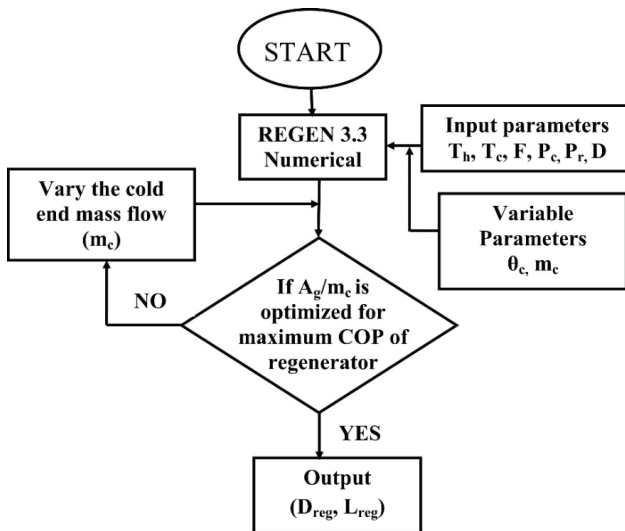


Figure 5. Systematic procedure for optimizing regenerator geometry in REGEN 3.3.

parameters are varied for the simulated model to obtain the maximum COP of the regenerator. A detailed discussion of the methodology employed by REGEN 3.3 is available in the software's user guide [33]. To systematically optimize the regenerator using REGEN 3.3, we employ the algorithm illustrated in Figure 5 following the methodology demonstrated in the previously published work [27]. All the simulations are carried out for various mass flows and phase angles at the cold end for fixed regenerator dimensions i.e. diameter and length. Further, the simulation case runs are repeated for different regenerator lengths to predict the optimal coefficient of performance. The same iterative procedure is repeated for all the geometrical and operating parameters to determine the optimal values of these variables for the maximum COP of a regenerator. The computational time required for each simulation in REGEN 3.3, given the above-selected range of parameters, is approximately 4 to 5 hours on a personal computer.

Validation of the Model

To validate the numerical procedure in REGEN 3.3, we conducted a comparison with previously published studies. Initially, we simulated a model using the same numerical data as Pfothenhauer et al. [27] to verify accuracy. Additionally, we simulated the regenerator model using the same data from Garaway et al. [36], who provided regenerator dimensions and experimentally tested the results. The spatial and temporal data comprised 41 mesh points, 200 time steps per cycle, and 30,000 cycles. The simulation results, obtained with the specified geometrical and operating data, agree with the published results and are presented in Table 1.

Regenerator Analysis

In this investigation, we examined the regenerator of an MPTC to enhance compactness and improve performance. We utilized REGEN 3.3 to optimize geometric dimensions and various operating parameters. The SS 635# wire mesh screen was chosen as the regenerator filler material due to its optimal pore size, porosity, and reliability across the cryogenic temperature range of 300 K to 80 K, as detailed in Table 2. However, the hydraulic diameter of the SS 635# screen limits the MPTC system's operating frequency to 200 Hz due to thermal penetration depth constraints. As a result, we fixed the parameters of the wire mesh screen and focused on optimizing other parameters within this constraint. Geometric dimensions and additional fixed and variable parameters are listed in Table 3.

Thermo-physical properties of the working gas (He-4) and the matrix materials selected as temperature-dependent properties. Based on the previously published data, the conductivity factor for the SS 635 # wire mesh screen was 0.13 for all the cases. One of the assumptions for all the simulated case runs is that the compressor impedance matched with the system.

Grid and Time Independence Study

A numerical model can reach a cyclic steady state after completing a simulation. To ensure the results' accuracy,

Table 1. Validation results for cryocooler regenerator

Parameters	Pfothenhauer et al. [27]	Present work	Error (%)	Garaway et al. [36]	Present work	Error (%)
COP	0.1318	0.1364	3.37	0.105	0.1103	4.8
NTCAD	-	-	-	1 W	1 W	-
PV power	-	-	-	13.35	13.5	1.11

Table 2. Geometric properties of the regenerator

Sr. No.	Regenerator Matrices	Wire Diameter (μm)	Hydraulic Diameter (μm)	Porosity (φ)
1.	SS 635 # Screen	20.3	30.58	0.6014

Table 3. Operating parameters for optimization of regenerator

Sr. No.	Parameters	Values	Unit
1.	Hot End Temperature (T_h)	300	K
2.	Cold End Temperature (T_c)	80	K
3.	Cooling Power (Q_{net})	1	W
4.	Regenerator Tube Internal Diameter (D)	4, 4.5, 5.0, 5.5, 6	mm
5.	Tube Thickness (t)	0.1	mm
6.	Frequencies (F)	100, 120, 140, 160, 180, 200	Hz
7.	Charge Pressure (P_c)	3.5, 4.0, 4.5, 5.0, 5.5, 6.0, 6.5, 7.0	MPa
8.	Pressure Ratio (Pr) at the cold end	1.15, 1.2, 1.25, 1.3	-

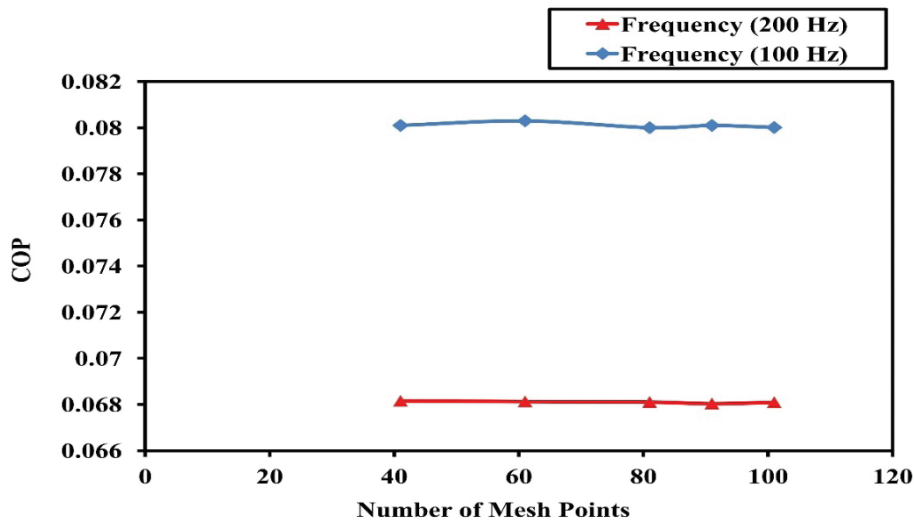


Figure 6. COP as a function of Number of Mesh Points for $D=4$ mm and $L=30$ mm, $N_{cycles}=10,000$, $m_c=0.0004$ Kg/s case 1: ($F=100$ Hz) (θ_c) = -25° Case 2: ($F=200$ Hz) (θ_c) = -35° .

the user needs to define certain parameters such as the number of iterations, grid points, and time steps used in each cycle. The regenerator simulation was started with an initial guess of 41 grid points, 100-time steps per cycle, and 1000 iteration conditions.

Figure 6 displays a mesh independence study with two different sets of conditions. In both of the two cases, the diameter is 4 mm and length is 30 mm, the mass flow at the cold end is (m_c) = 0.0004 kg/s, the number of cycles is 10,000, the number of time steps per cycle is 250, and the midpoint temperature ratio is 0.45. The value of phase angle at the cold end and frequency for Case 1 and 2 are (θ_c) = -25° , $f_1=100$ Hz & (θ_c) = -35° , $f_2=200$ Hz, respectively. The study reveals that very little variation is observed in both cases with higher grid points over 81. The variation obtained in COP is 0.0115 % & 0.0145 % for case no. 1 & 2

respectively. Hence for all the further simulations, 81 mesh points are selected.

Figure 7 displays how the COP of the system changes with the number of time steps per cycle. The analysis was performed on a regenerator with a diameter of 4 mm, length of 25 mm, a frequency of 100 Hz, 10,000 numbers of cycles, and a midpoint temperature ratio of 0.45. When the time step is varied from 100 to 250, COP variation was found 7.67 %, but only 0.98% variation was found when increased from 250 to 450. Thus, a value of 250 time steps per cycle is selected for temporal discretization in further simulations to reduce the run time. Further, for both cases, dependency on various cycles has been studied, and the result reveals that by increasing the final number of cycles from 10,000 to 30,000, the solution produces very little error (i.e.) 0.01 %, while the case run time reduces significantly.

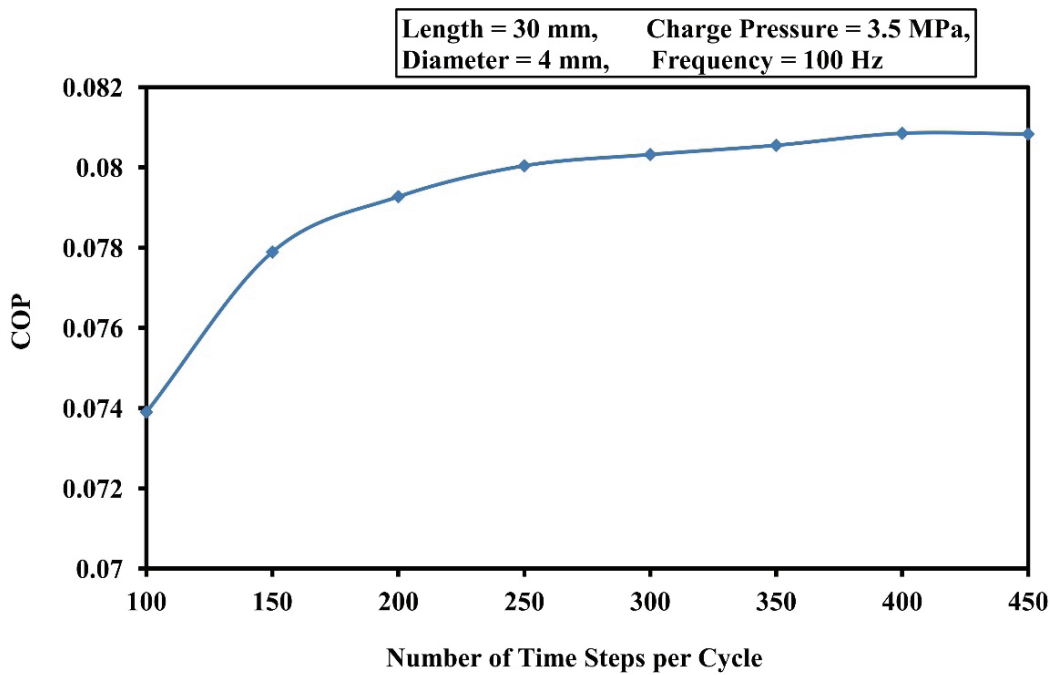


Figure 7. Effect of time steps per cycle on COP.

RESULTS AND DISCUSSION

Numerical models have been developed using REGEN 3.3 to examine how various operating parameters affect the performance over temperatures ranging from 300 K and 80 K.

Figure 8 shows the graphical output of a simulated case run using REGEN 3.3 software. The graph displays the cell energy balance within the gas, indicating that the energy

flux through the cell walls and the heat exchange between the gas and the matrix significantly influence the rate of change of energy in the gas contained within the cell. The graph features four functions that define the energy balance in the cell. The first function shows the rate of change (DT (ENG)) over the time step of the energy of the gas contained in the cell (W). The second function shows net enthalpy and conductive flux (DX (ENT)) (W) through the ends of the cell. The third function shows the average heating rate

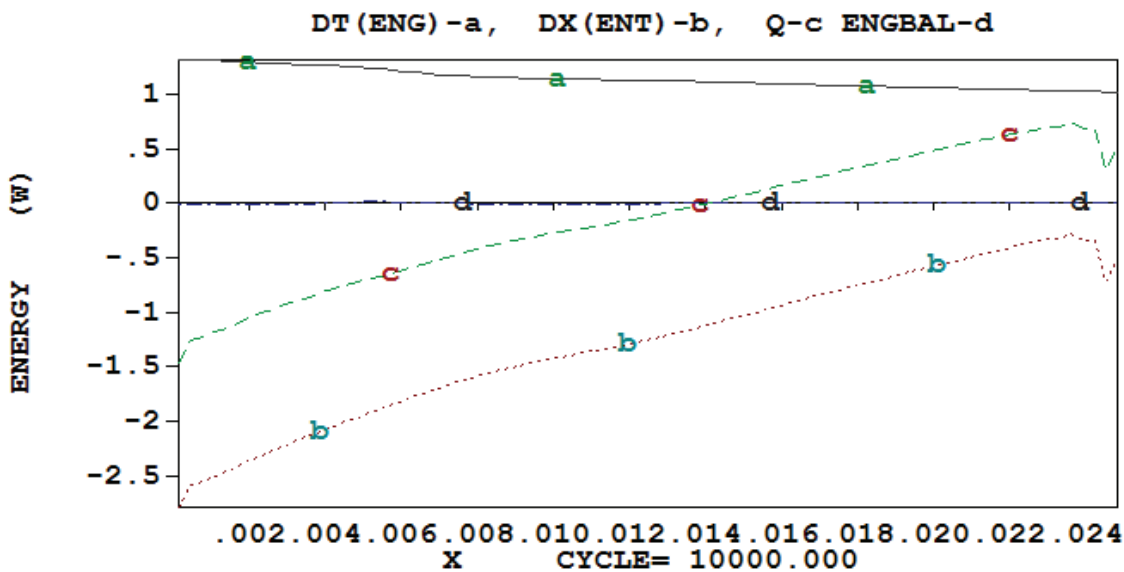


Figure 8. Cell energy balance in the gas.

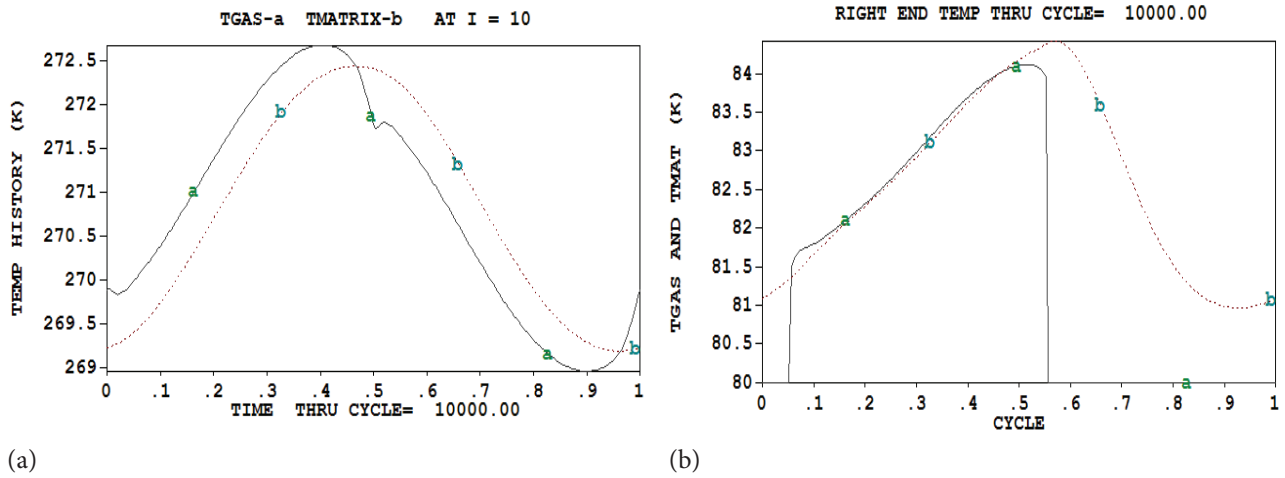


Figure 9. Instantaneous Gas and Material temperatures at the ends of the regenerator (a) hot end (b) cold end.

(Q) (W) from the gas to the matrix over the time step. The last curve (BAL) is the energy balance over the cell (W), which would vanish if the computation was perfectly accurate. In the present simulation, the energy balance in the cell approaches zero, indicating a high degree of accuracy.

Figure 9 illustrates the temporal variation of gas (TGAS) and matrix (TMAT) temperatures (K) at both the hot and cold ends of the regenerator throughout the cycle. This figure demonstrates the dynamic thermal behavior, with the gas temperature fluctuating more rapidly than the matrix due to its lower thermal mass and faster response time. The phase angle between TGAS and TMAT is crucial for effective heat transfer; ideally, when TGAS reaches its peak, TMAT should be at a lower temperature. This relationship

indicates that the matrix's thermal inertia allows it to absorb and release heat efficiently, enhancing the overall cooling efficiency of the system.

Figure 10 shows the average gas and matrix temperature plotted as a function of distance along the regenerator. The value at each mesh point is averaged over the cycle. The overlap of the temperature profiles indicates effective heat transfer and balanced thermal conditions within the regenerator. The temperature gradient shows that as the gas flows through the regenerator, it cools down while the matrix absorbs heat, leading to a gradual increase in its temperature.

Figure 11 shows three curves of pressure (Pa) versus the volume of the regenerator. The first curve (HOT-V-a)

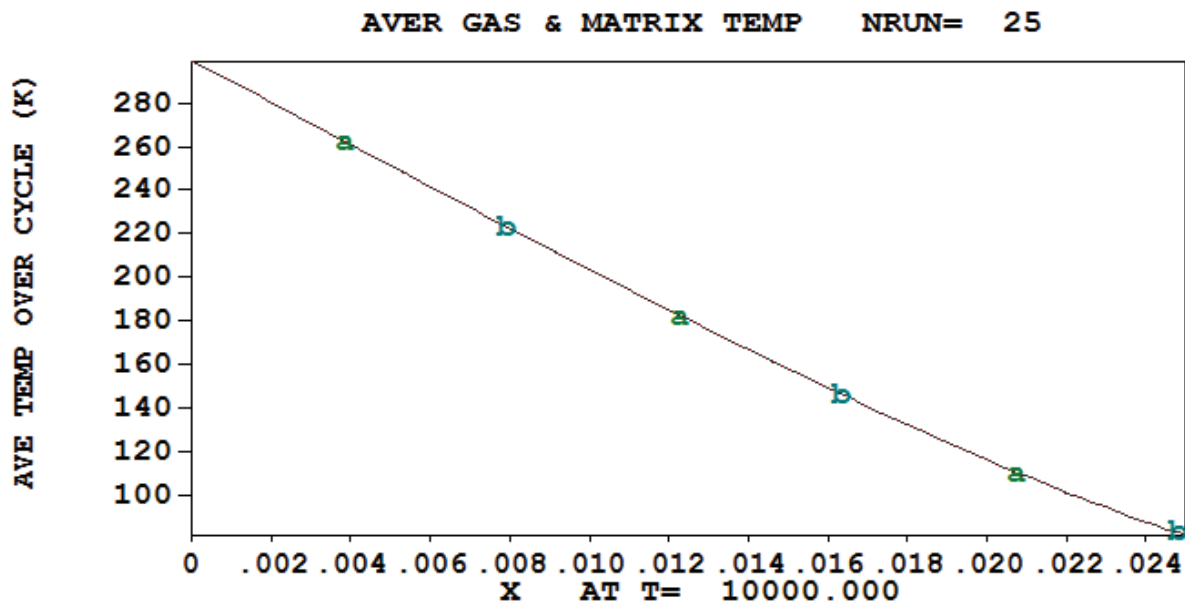


Figure 10. The temperature profile of the gas and the material along the length of the regenerator at 100 Hz.

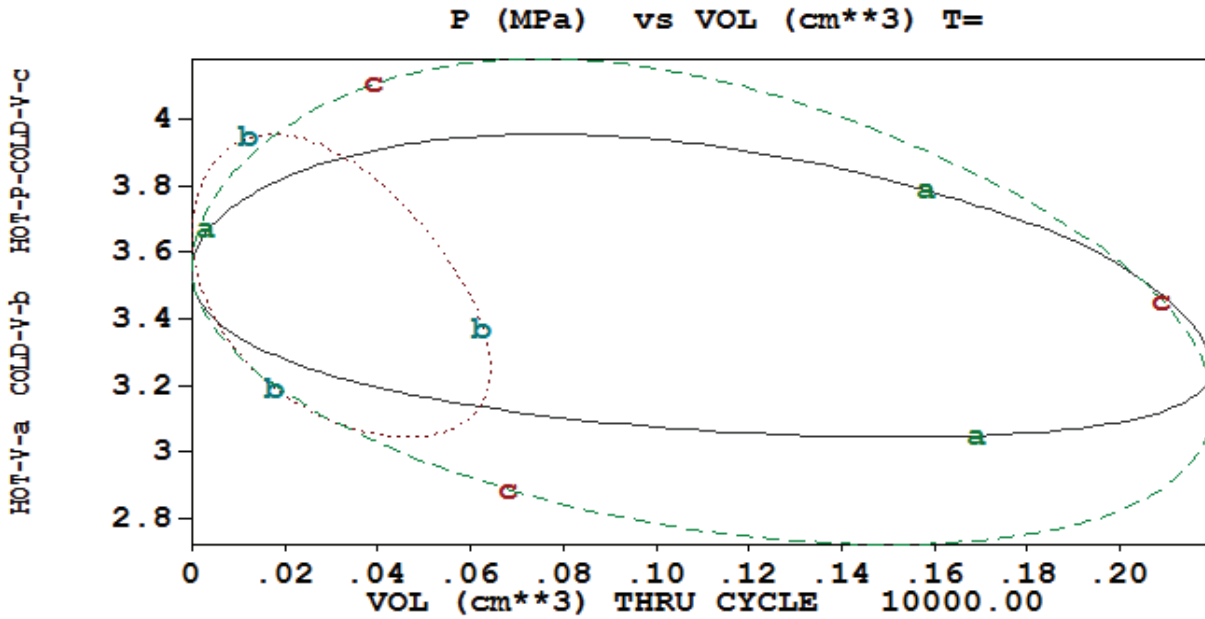


Figure 11. The pressure-volume (PV) diagram at both the hot and cold ends of the regenerator for an operating frequency of 100 Hz.

is the cold end pressure plotted against the compression volume. As compression increases, the pressure at the cold end decreases, primarily due to the reduced temperature, which lowers the gas density and pressure. The second curve (COLD-V-b), is the pressure at the cold end plotted against the expansion volume. Here, the pressure at the cold end increases with expansion volume, as the gas absorbs heat during expansion, leading to higher pressure. The third curve (HOT-P-COLD-V-c), is the pressure at the hot end including the pressure drop plotted against the

compression volume. This curve shows the pressure drop at the hot end due to frictional losses and heat dissipation within the regenerator. The PV diagram reveals that the associated with the cold end is smaller than the hot end due to reduced volume with temperature.

Figure 12 contains two curves (PHOT-a) and (PCOLD-b) that show the pressure as a function of time at the hot and cold ends of the regenerator. In REGEN 3.3 the pressure at the hot end is corrected to include the pressure drop as computed from the correlation. The pressure

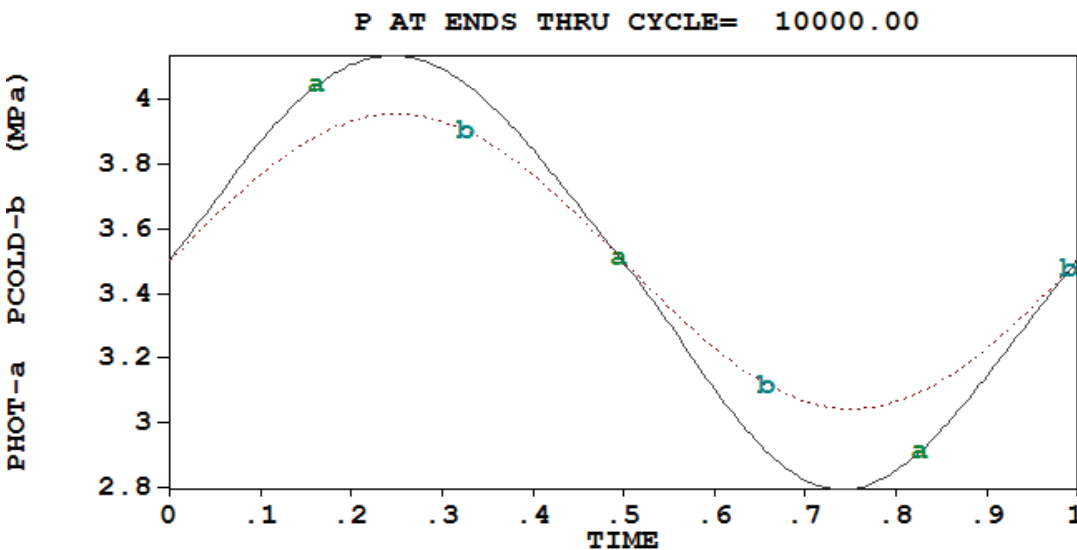


Figure 12. Pressure (Pa) over time at the hot and cold ends of the regenerator at 100 Hz.

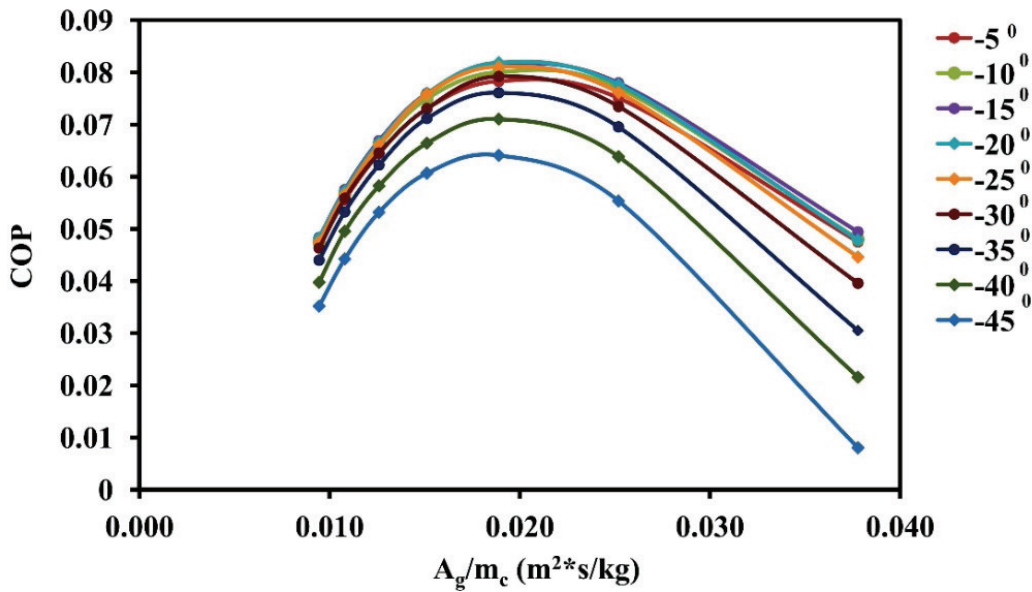


Figure 13. COP versus inverse mass flux (A_g/m_c) at various cold end phase angles (θ_c).

amplitude at the hot end of the regenerator is greater than that at the cold end, primarily due to the pressure drop that occurs along its length. This drop arises from resistance to flow and thermal conduction effects as the working fluid travels through the regenerator. Energy loss from viscous interactions with the internal surfaces contributes to a decrease in pressure by the time the fluid reaches the cold end.

Figure 13 presents the COP plotted against inverse mass flux (A_g/m_c) and cold end phase angle for a case of $P_c = 3.5$ MPa, $P_r = 1.3$, $T_h = 300$ K, $T_c = 80$ K, $F = 100$ Hz, and $L = 25$ mm. The graph depicts that there is an optimal phase angle and inverse mass flux at which the cryocooler produces

maximum COP. The maximum COP of 0.0819 is obtained at 0.019 m²/s/kg inverse mass flux and $\theta_c = -20^\circ$. These values of inverse mass flux and phase angle are well matched with those reported in the literature for similar wire mesh screens operating at frequencies between 100 Hz and 200 Hz [27, 36]

Figure 14 represents the COP over a range of inverse mass flux for a $T_h = 300$ K, $T_c = 80$ K, charge pressure (P_c) = 3.5 MPa, $P_r = 1.3$, $F = 100$ Hz, and 200 Hz. It is seen that for the given range of mass flux; COP for 100 Hz is always larger than the 200 Hz frequency. It is observed that the higher frequency requires a smaller mass flux to obtain the maximum COP, demonstrating the increased sensitivity

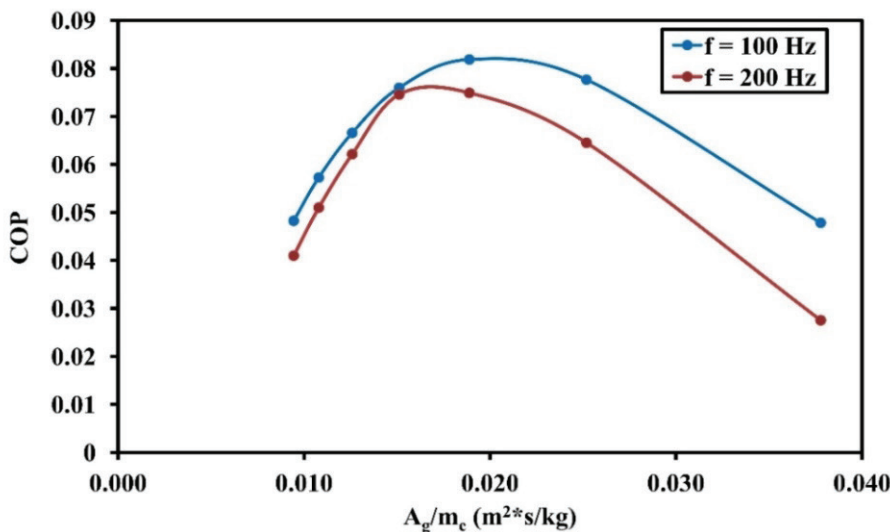


Figure 14. COP variation with inverse mass flux (A_g/m_c) at optimized cold end phase angle (θ_c) for 100 and 200 Hz.

of the system's efficiency to changes in operational frequency and mass flux. This result follows similar trends as in the literature [27], which demonstrated that lower operational frequencies enhance thermal interactions, thereby improving the overall efficiency of the system.

Effect of Frequency

The effect of frequency on the optimized regenerator dimensions is studied by simulating the same data set but with different operating frequencies.

Meanwhile, at 200 Hz, the regenerator's optimized dimensions are 4 mm in diameter and 20 mm in length, with a COP of 0.07491. It is observed from the generated data that for an optimized dimension at 100 Hz, the COP value decreases by 9.768% when the operating frequency is increased from 100 Hz to 200 Hz. Under identical conditions, with a regenerator diameter of 4 mm, when the regenerator length is 20 mm, the COP decreases by 5.093% compared to the optimized length of 25 mm. Furthermore, at a length of 30 mm, it undergoes a decrease of 14.91%

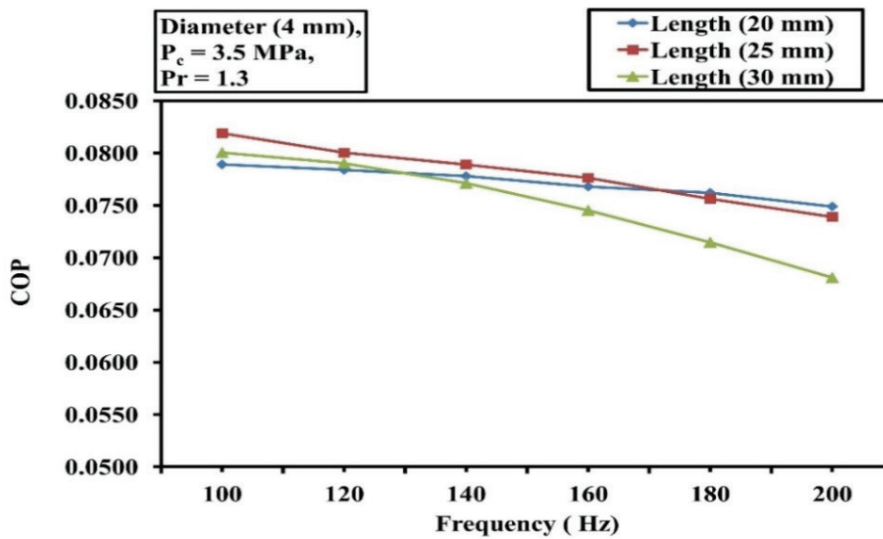


Figure 15. Frequency vs. COP for D = 4 mm, Pc = 3.5 MPa, Pr = 1.3, Tc = 80 K.

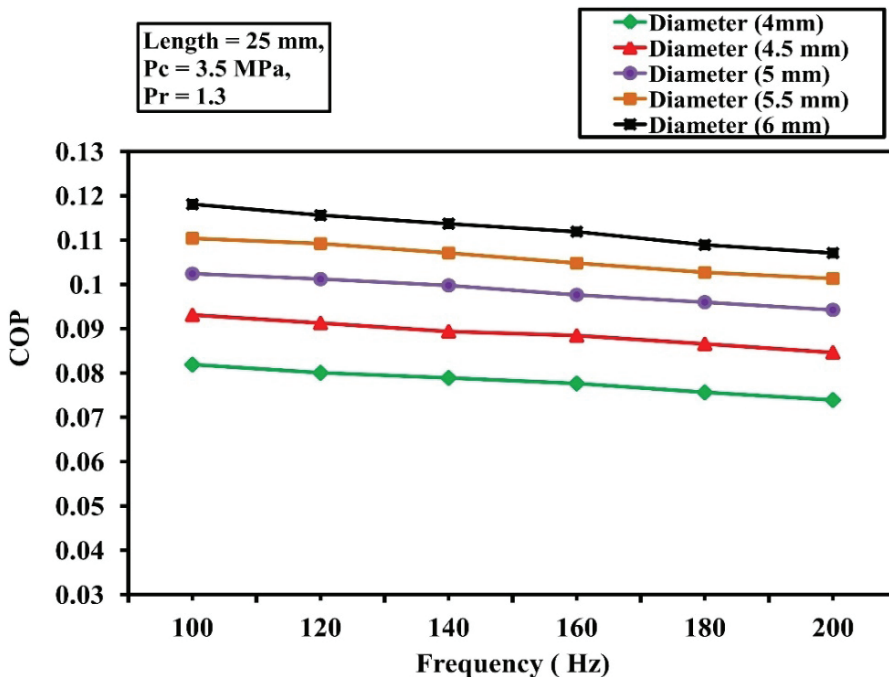


Figure 16. Frequency vs. COP for L = 25 mm, Pc = 3.5 MPa, Pr = 1.3, Tc = 80 K.

compared to the optimized length of 25 mm. When the frequency is increased from 100 Hz to 200 Hz, the length of the regenerator at the optimized diameter of 4 mm is shortened by 20 %, reducing from 25 mm to 20 mm. Simultaneously, the coefficient of performance (COP) decreases by approximately 8.51%, shifting from 0.0819 to 0.07491. This observed deviation in the COP value at a high frequency of 200 Hz is consistent with findings that suggest an oversized regenerator can lead to increased pressure drops and temperature oscillations [2]. These factors contribute to reduced thermal performance, highlighting the importance of optimizing the regenerator’s dimensions to maintain efficiency under varying operational conditions.

Figure 16 shows the influence of frequency on the fixed length and variable diameter across the same range of mass flux and cold end phase angle under the specified conditions of $T_h = 300$ K, $T_c = 80$ K, $P_c = 3.5$ MPa, $Pr = 1.3$. For fixed operating parameters when the optimal diameter was reduced from 6 mm to 4 mm, the value of COP decreased by 30.65 %, and for 200 Hz, the value of COP decreased by 30.99 %. The decrease in diameter results in a proportionate reduction in the cross-sectional area available for the heat transfer within the regenerator. As a result, the overall heat transfer area becomes smaller, limiting the regenerator’s ability to efficiently exchange thermal energy with the working fluid. With a smaller optimal diameter, the heat transfer process becomes insufficient within the regenerator. The diminished diameter affects the effectiveness of the heat transfer process, leading to decreased overall

performance. For a fixed geometrical and operating condition, the value of COP reduces uniformly with the increase in frequencies. The uniformity of this reduction emphasizes the relationship between frequency and COP under the specified conditions.

Figure 17 shows the effects of frequencies on various losses and ineffectiveness of the regenerator. As the operating frequency increases from 100 Hz to 200 Hz, the gas oscillation rate within the regenerator also increases. This results in higher average gas velocities and higher turbulence. The increased turbulence raises the resistance to flow, which leads to a 25% increase in pressure drop through the regenerator. Previous studies [10] observed similar trends but focused on a narrower frequency range of 40 Hz to 60 Hz. Our study extends this by examining a range of 100 Hz to 200 Hz, providing a clearer understanding of how frequency impacts flow resistance and overall performance. Additionally, higher frequencies reduce the thermal penetration depth, causing thermal waves to penetrate less deeply into the regenerator material. The reduction in thermal penetration depth enhances heat transfer within localized regions of the regenerator. As a result, despite the increase in pressure drop with higher frequency, there is no significant variation in ineffectiveness and regenerator losses, thereby preserving overall system efficiency.

Effect of Charge Pressure

To investigate the effect of charge pressure on the optimized regenerator dimensions employing a constant dataset while varying operating frequencies through simulations.

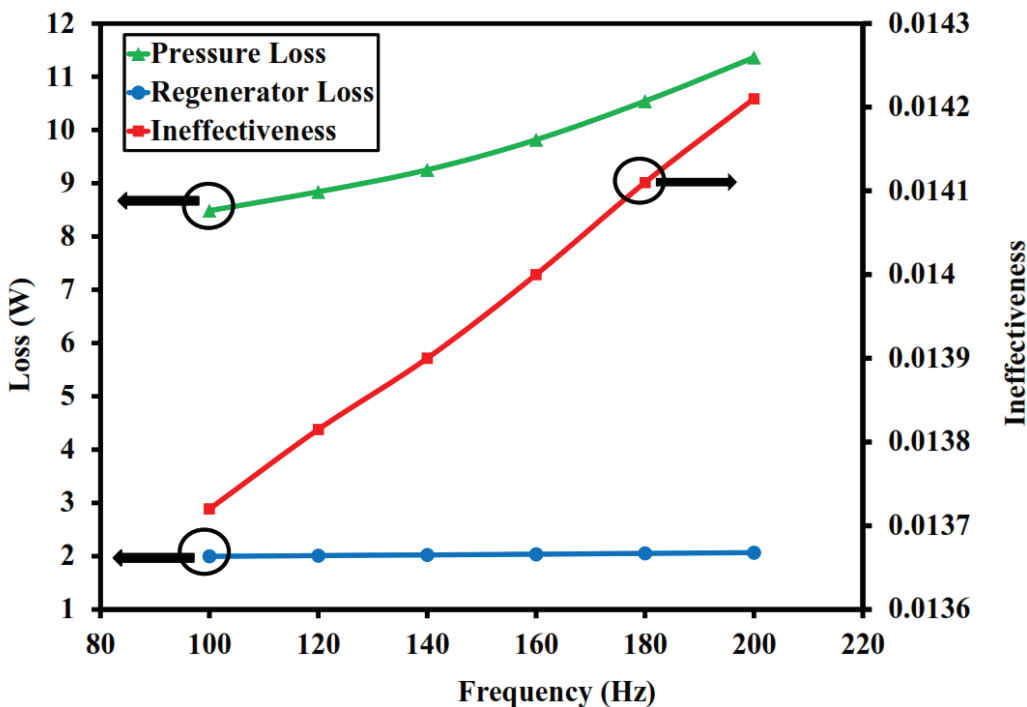


Figure 17. Effects of frequencies on losses and ineffectiveness.

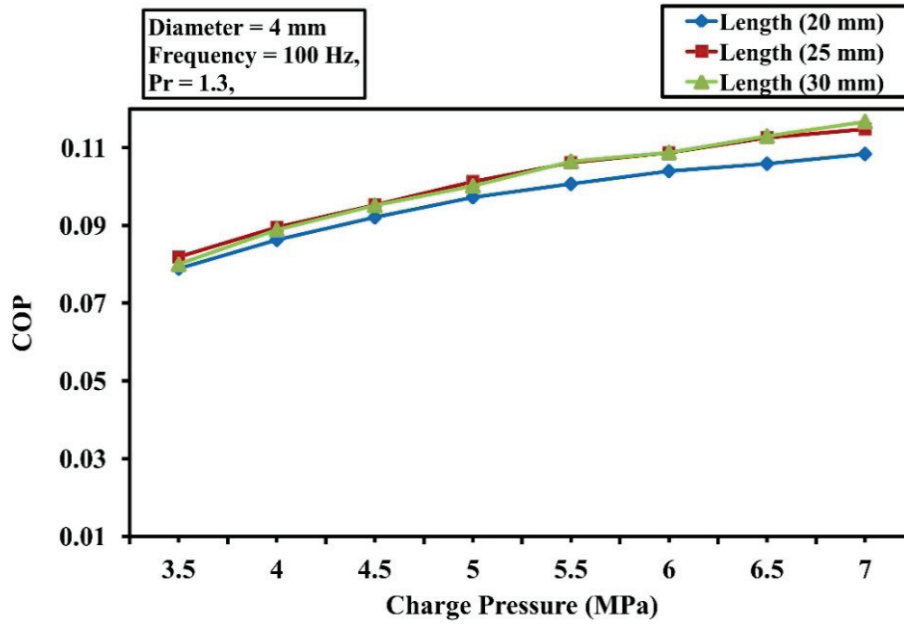


Figure 18. Charge pressure vs. COP for D 4 mm, Pr = 1.3, F = 100 Hz, T_c = 80 K.

Figure 18 represents the effect of charge pressure on the optimized regenerator dimension. It is observed that the COP of the system improves as the charge pressure increases for a given diameter and length. This effect is attributed to the higher power density and increased mass flow amplitude at the cold end of the regenerator. With the change in regenerator length from 30 mm to 20 mm, only a 1.4% reduction is observed for a charge pressure of 3.5 MPa, and a 7.11% reduction is observed for 7.0 MPa. However, there is no substantial effect of charge pressure seen on optimized length. This indicated that, beyond a certain point,

additional increases in charge pressure result in no significant improvements in length optimization, indicating that the optimal regenerator length remains almost constant across various charge pressures.

Figure 19 represents the effect of charge pressure on regenerator diameter and length over the same ranges of mass flux and cold end phase angle with the case of T_h = 300 K, T_c = 80 K, Pr = 1.3, and f = 100 Hz & 200 Hz. When the regenerator diameter reduced from 6 mm to 4 mm for a charge pressure of 3.5 MPa and 7.0 MPa, the COP decreased by 32.43 % and 20.55% for 100 Hz, 30.78%, and 20.59% for

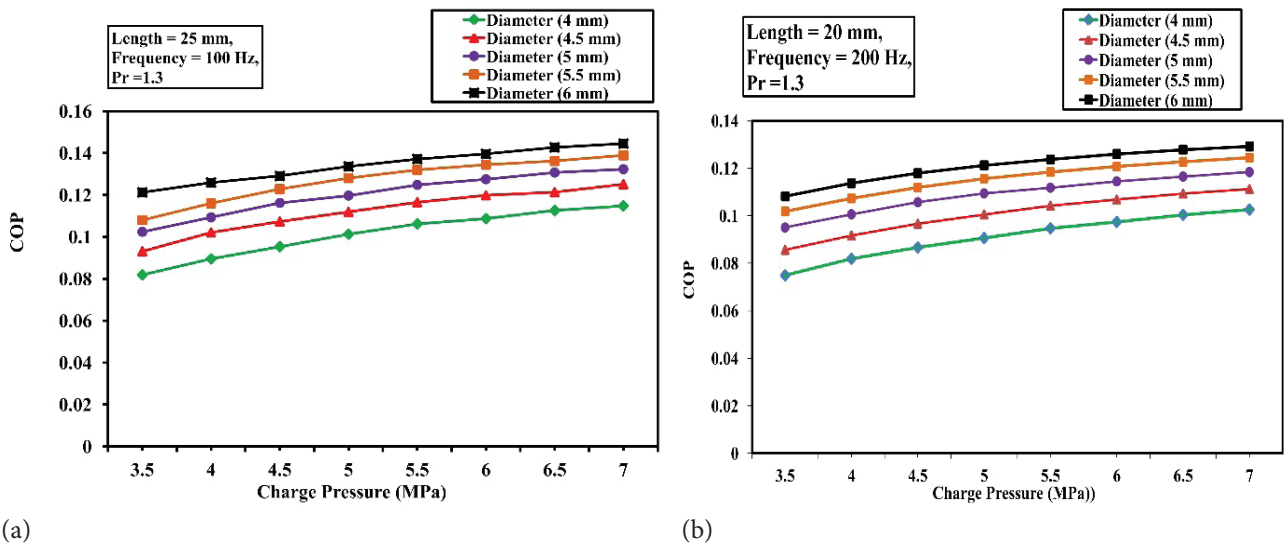


Figure 19. Charge pressure vs. COP for Pr = 1.3, T_c = 80 K over various diameters at operating frequencies (a) f = 100 Hz (b) f = 200 Hz.

200 Hz, respectively. The trend is due to the smaller regenerator diameter limiting the mass flow of gas, which reduces heat transfer, and overall performance. For an optimized regenerator dimension at a frequency of 100 Hz, the COP increases by 28.65 % with the increase in charge pressure from 3.5 MPa to 7.0 MPa, and for a frequency of 200 Hz, the COP increases by 26.99%. As pressure ratios increase, the regenerator’s effectiveness improves due to a more uniform temperature distribution, which reduces temperature gradients and enhances thermal interactions between helium gas and regenerator material. This uniformity also minimizes dead volume effects, where heat transfer is less efficient.

Figure 20 represents the influence of charge pressure on various losses and the ineffectiveness of the regenerator. Miniature pulse tube cryocooler performance improves significantly when the charge pressure of helium gas increases from 3.5 MPa to 7.0 MPa. This higher pressure increases the density and thermal conductivity of the helium gas, thus leading to more efficient heat transfer within the regenerator and a reduction in thermal resistance, preventing significant increases in regenerator losses. Additionally, the higher pressure reduces the thermal penetration depth, further enhancing thermal performance. Moreover, the increased pressure alters the acoustic impedance of the system, which promotes a more favorable interaction between the gas flow and the regenerator, reducing frictional losses and achieving a notable 73% reduction in pressure drop across the regenerator.

Effect of Pressure Ratio

To investigate how the pressure ratio influences the optimized regenerator dimensions, a constant dataset was used while varying operating frequencies through simulations. To investigate the impact of pressure ratio on the optimized regenerator dimensions in an MPTC, simulations are conducted with varying operating pressures while keeping the remaining set of data consistent.

Figure 21 depicts the effect of pressure ratio on the optimized diameter and variable length over the same mass flux range and cold end phase angle with the case of $T_h = 300$ K, $T_c = 80$ K, $P_c = 3.5$ MPa, and F 100 Hz. When the regenerator length decreased from 30 mm to 20 mm for pressure ratios of 1.15 and 1.3, the COP reduced by 59.24 % and 5.37 %. At lower pressure ratios, deviations from the optimal regenerator length significantly impact the coefficient of performance due to reduced gas density and thermal inertia, requiring longer regenerators for effective heat exchange. In contrast, at higher pressure ratios, increased gas density enables shorter regenerator lengths without significant performance loss. For an optimized diameter and length at a frequency of 100 Hz, the COP increases by 80.75 % with the increase in pressure ratio from 1.15 to 1.3. This significant improvement emphasizes how higher-pressure ratios lead to greater gas density and better thermal interaction within the regenerator. It is also seen that at an optimized diameter; the length of the regenerator can be reduced with the increase in the pressure ratio.

Figure 22 shows that increasing the pressure ratio within the specified data range enhances the performance

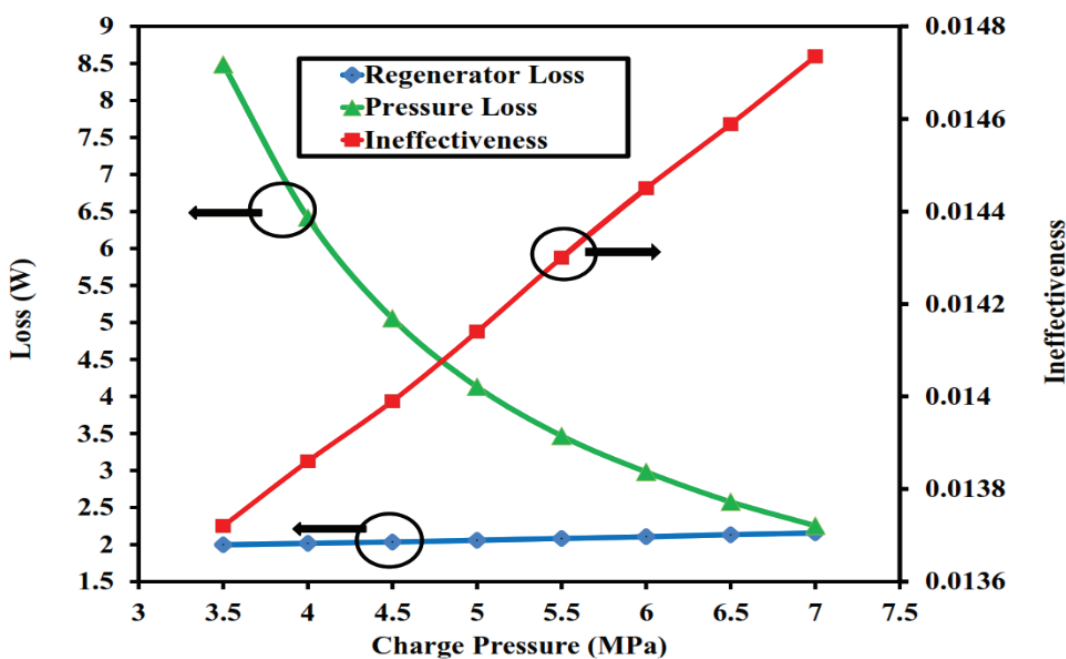


Figure 20. Effects of charge pressure on losses and ineffectiveness.

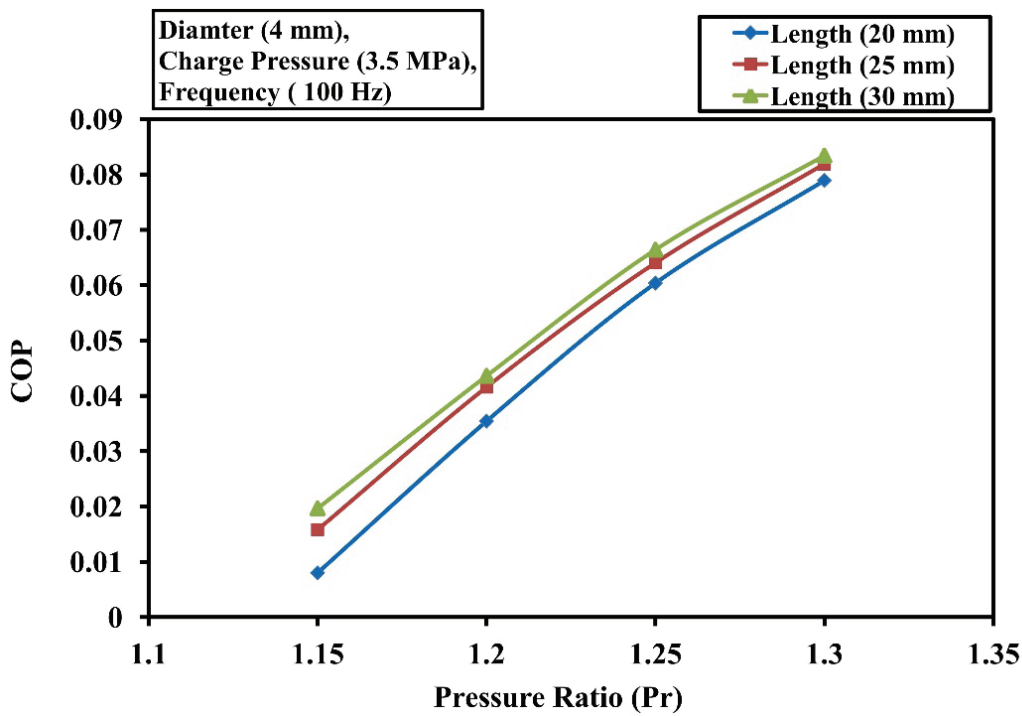


Figure 21. Pressure ratio vs. COP for $D = 4 \text{ mm}$, $P_c = 3.5 \text{ MPa}$, $f = 100 \text{ Hz}$, $T_c = 80 \text{ K}$.

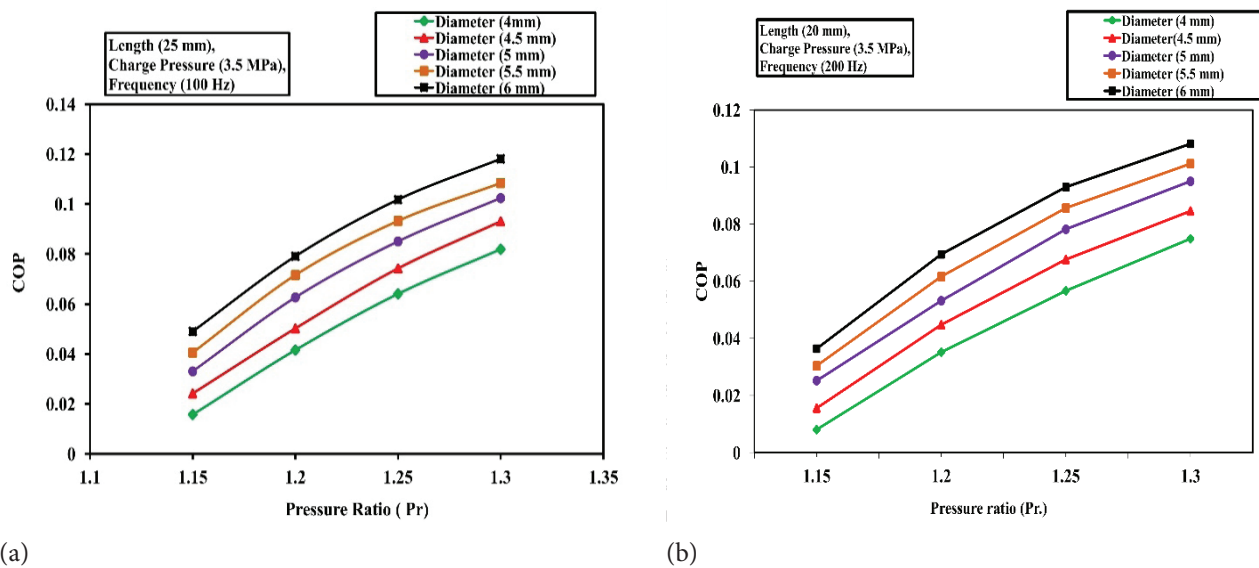


Figure 22. Pressure ratio vs. COP at $P_c = 3.5 \text{ MPa}$, $T_c = 80 \text{ K}$ over various diameters at operating frequencies (a) $f = 100 \text{ Hz}$ and (b) $f = 200 \text{ Hz}$.

of the MPTC. When regenerator diameters are reduced from 6 mm to 4 mm for a pressure ratio ranging from 1.15 to 1.3, the COP decreases by 67.83 % and 30.65% for 100 Hz, and 200 Hz reduces by 59.25% and 10.3%. The COP shows a linear variation within the pressure ratio under fixed geometry and operating conditions. Additionally, an increase in pressure ratio allows for the reduction of the

regenerator diameter, maintaining an optimized length due to improved system efficiency and pressure drop management. Higher pressure ratios improve the thermodynamic efficiency of MPTCs, allowing the system to handle larger pressure drops. This is because a higher pressure ratio maximizes the temperature differential across the system, which enhances heat transfer efficiency. The significant decrease

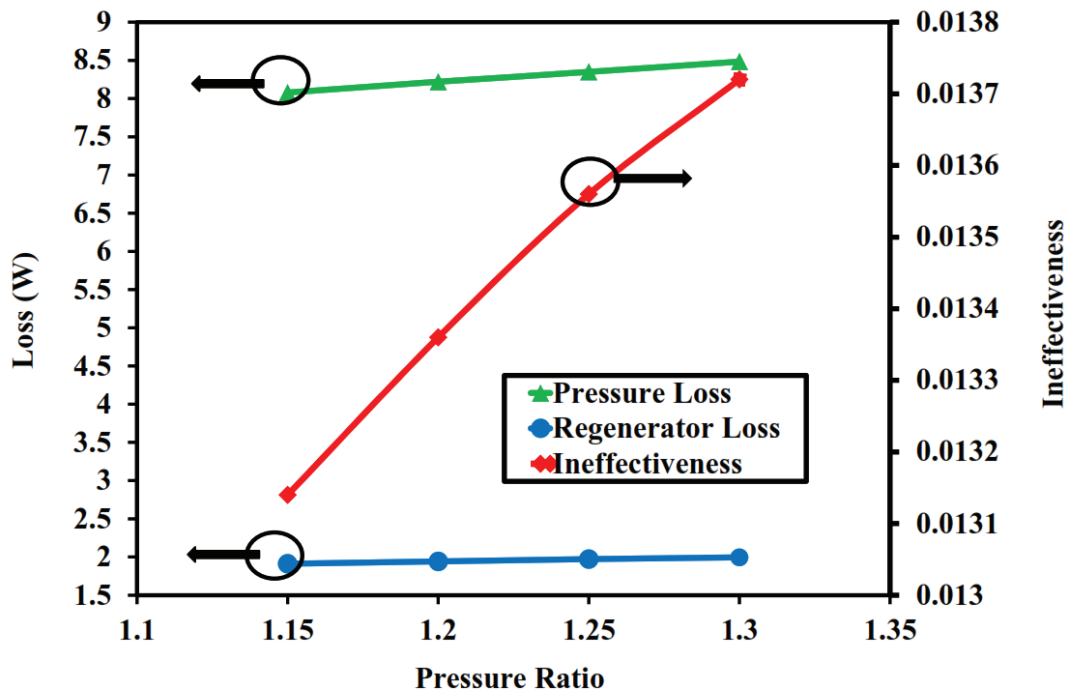


Figure 23. Effects of pressure ratio on losses and ineffectiveness.

in COP with reduced regenerator diameter suggests that while smaller regenerators can contribute to a more compact design, they may also increase the flow resistance and lead to decreased effectiveness. Therefore, optimizing the pressure ratio and regenerator geometry is essential to ensure that performance is maintained without significant losses.

Figure 23 shows the effects of pressure ratios on various losses and ineffectiveness of the regenerator. Increasing the pressure ratios from 1.13 to 1.3 improves the density of helium gas, which in turn enhances its thermal conductivity. This improved conductivity facilitates better heat transfer within the regenerator, helping to reduce potential pressure drop losses. As the depth of thermal penetration decreases, heat is transferred more efficiently within specific areas of the regenerator. Consequently, this enhanced heat transfer efficiency helps minimize the overall effect on performance. At higher pressure ratios, the effectiveness of the regenerator improves due to a more uniform temperature distribution, which improves heat transfer efficiency between the gas and the regenerator material. This optimization further reduces the effects of dead volume, where heat transfer is less efficient, leading to significant performance enhancements.

CONCLUSION

The numerical investigations in the present study focused on the design and optimization of the regenerator, to improve performance at ultra-high frequencies and

maximize the coefficient of performance. This study presents a novel approach by addressing the underexplored challenges of ultra-high frequency operation in miniature pulse tube cryocoolers, offering new insights and optimization strategies essential for developing more efficient and compact systems. The study systematically examined the effects of regenerator structural dimensions and operating parameters on the coefficient of performance.

The key geometrical parameters considered in this paper are the diameter and length of the regenerator, while the operating parameters include ultra-high frequencies (100 Hz-200 Hz), charge pressures (3.5 MPa-7.0 MPa), and cold-end pressure ratios (1.15-1.3). In the study, the parameters are optimized to maximize the coefficient of performance and achieve 1 W cooling at 80 K. The main findings are summarized as follows:

Regenerator Dimensions and Frequency Effects:

1. At 100 Hz, the optimal regenerator dimensions are a diameter of 4 mm and a length of 25 mm, which results in a coefficient of performance of 0.0819.
2. At 200 Hz, with the same diameter but a reduced length of 20 mm, the coefficient of performance reduces to 0.07491. This trend indicates that the regenerator performance deteriorates with increasing operating frequency, even when the dimensions are optimized.
3. Increasing the frequency from 100 Hz to 200 Hz, while maintaining optimal regenerator dimensions, results in a 9.768% decrease in the coefficient of performance and a 20% reduction in the regenerator length. Thus, we can conclude that the working frequency has little influence

on the optimal diameter, while the regenerator length can be reduced under certain conditions.

Effect of Charge Pressure:

1. With optimized diameter and length, the coefficient of performance improves by 28.65 % at a frequency of 100 Hz when the charge pressure is increased from 3.5 MPa to 7.0 MPa and increases by 26.99 % at 200 Hz. However, charge pressure has little effect on the regenerator's optimum dimensions.

Effect of Pressure Ratio:

1. For an optimal diameter and length, the coefficient of performance increased by 80.75% with an increase in pressure ratio from 1.15 to 1.3. The higher the cold end pressure ratio, the shorter the optimal length of the regenerator, and the smaller the path.
2. The performance of the regenerator of a miniature pulse tube cryocooler improves with the increased charge pressure and pressure ratio. The optimized regenerator dimension is independent of the charge pressure and dependent on the cold end pressure ratio.

To achieve the best performance of the regenerator in a miniature pulse tube cryocooler, it is essential to select the optimal regenerator size and strategically increase both charge pressures and pressure ratios. By improving thermal performance in compact designs, our results address the requirements for high efficiency and reduced size, weight, and power requirements essentials for cryogenic cooling in satellite applications, particularly for infrared sensors used in Earth Observation and surveillance. This work enhances the reliability and effectiveness of the system, which are critical for ensuring the optimal functionality of satellite instruments. Moreover, these results can also be used for ultra-high frequency Stirling cryocoolers.

The most prominent feature of the present study is the capability to design an ultra-high-frequency regenerator that operates at high efficiency while maintaining compact dimensions. Due to the high cost and complexity of prototype testing at these frequencies, this research relied on numerical simulations using REGEN 3.3. Future work will focus on validating these findings through experimental testing as resources and facilities become available.

NOMENCLATURE

A	Cross-sectional Area, m^2
D	Diameter, m
D_h	Hydraulic diameter, m
d_w	Wire diameter, m
t	Tube thickness, m
L	Tube Length, m
C_m	Heat capacity, J/m^3k
E	Total Energy, J/m^3
$H(p, T, \nu)$	Heat transfer rate between the gas and the matrix, $W / m.K$
$k_g(p, T)$	Thermal conductivity of the matrix material, $W / m.K$

$p(t)$	Pressure, Pa
Pr	Pressure ratio
$p_d(t)$	Instantaneous dynamic pressure
T_c	Cold-end gas inflow temperature, K
T_h	Hot-end gas inflow temperature, K
T_m	Temperature of the matrix material, K
t	Time, sec
x	Spatial coordinate, 0
	Velocity of the gas, m/s
ν	Velocity of the gas, $0 \leq x \leq L$, m
	Greek symbols
$\rho(p, T)$	Density of the working gas, kg/m^3
τ	Period of oscillation, s
ϕ	Porosity
$\sigma(T)$	thermal conductivity of stainless steel
	Subscripts
m	Refers to matrix
c	Refers to cold end temperature of gas
h	Refers to the hot end temperature of the gas

Abbreviation

PTC	Pulse Tube Cryocooler
MPTC	Miniature Pulse Tube Cryocooler
NIST	National Institute of Standards & Technology
COP	Coefficient of Performance
CFD	computational fluid dynamics
NTCAD	Net Cooling Power
pvwk _{0T}	Hot end pV work
PVWK ₁	Cold end pV work
GRCAD	Gross cooling power
rgloss	Loss due to regenerator ineffectiveness
PRLOSS	Correction term to estimate the effect of pressurization on the enthalpy flux of gas
TUBE_H	Tube thickness
COOLING_MULT	Multiplication Factor to reduce gross refrigeration power
ENTFLUX	Integral average of Enthalpy Flux at the right end of the regenerator over one cycle
TUBECD	Thermal Conduction through the tube containing the regenerator matrix

AUTHORSHIP CONTRIBUTIONS

Authors equally contributed to this work.

DATA AVAILABILITY STATEMENT

The authors confirm that the data that supports the findings of this study are available within the article. Raw data that support the finding of this study are available from the corresponding author, upon reasonable request.

CONFLICT OF INTEREST

The authors declared no potential conflicts of interest with respect to the research, authorship, and/or publication of this article.

ETHICS

There are no ethical issues with the publication of this manuscript.

REFERENCES

- [1] Radebaugh R. Pulse tube cryocoolers for cooling infrared sensors. Proceedings of SPIE, the International Society for Optical Engineering, Infrared Technology and Applications XXVI, Vol. 4130; 2000. pp. 363–379. [\[CrossRef\]](#)
- [2] Radebaugh R, Gallagher A. Regenerator operation at very high frequencies for microcryocoolers. AIP Conf Proc 2006;851:1919–1928. [\[CrossRef\]](#)
- [3] Dang H. Development of high frequency pulse tube cryocoolers for space applications. AIP Conf Proc 2012;1434:1457–1464. [\[CrossRef\]](#)
- [4] Vanapalli S, Gan Z, Radebaugh R. 120 Hz pulse tube cryocooler for fast cooldown to 50 K. Appl Phys Lett 2007;90:072504. [\[CrossRef\]](#)
- [5] Radebaugh R, Garaway I, Veprik AM. Development of miniature, high frequency pulse tube cryocoolers. In: Andresen BF, Fulop GF, Norton PR, eds. Infrared Technology and Applications XXXVI. Proceedings of SPIE Vol. 7660; 2010. [\[CrossRef\]](#)
- [6] Wang X, Yu L, Zhu J, Yu G, Dai W, Hu J, et al. A miniature coaxial pulse tube cooler operating above 100 Hz. Cryocoolers 2012;17:107–114.
- [7] Mohan S, Atrey M. Development of inline high frequency miniature pulse tube cryocooler for 80 K applications. Indian J Cryogenics 2014;39:175. [\[CrossRef\]](#)
- [8] Ouyang Y, Tang Q, Wang N, Liu X, Liang J. Research on 1 kg miniature pulse tube cryocooler. Cryocoolers 2018;18:103–107.
- [9] Bao D, Tan J, Zhang L, Gao Z, Zhao Y, Dang H. A two-dimensional model of regenerator with mixed matrices and experimental verifications for improving the single-stage Stirling-type pulse tube cryocooler. Appl Therm Eng 2017;123:1278–1290. [\[CrossRef\]](#)
- [10] Liu S, Jiang Z, Ding L, Zhu H, Huang Q, Wu Y. Impact of operating parameters on 80 K pulse tube cryocoolers for space applications. Int J Refrig 2019;99:226–233. [\[CrossRef\]](#)
- [11] Garg SK, Premachandran B, Singh M, Sachdev S, Sadana M. Effect of porosity of the regenerator on the performance of a miniature Stirling cryocooler. Therm Sci Eng Prog 2020;15:100442. [\[CrossRef\]](#)
- [12] Zhao Y, Yu G, Tan J, Mao X, Li J, Zha R, et al. CFD modeling and experimental verification of oscillating flow and heat transfer processes in the micro coaxial Stirling-type pulse tube cryocooler operating at 90–170 Hz. Cryogenics 2018;90:30–40. [\[CrossRef\]](#)
- [13] Malwe P, Gawali B, Dhalait R, Deshmukh NS. Performance analysis and exergy assessment of an inertance pulse tube cryocooler. J Therm Eng 2023;9:1–11. [\[CrossRef\]](#)
- [14] Abraham D, Kuzhiveli BT. Investigation of regenerator mesh characteristics for a pulse tube cryocooler. IOP Conf Ser Mater Sci Eng 2022;1240:012132. [\[CrossRef\]](#)
- [15] Guo ZM, Zhu SW. A research of micro-pulse tube cryocooler with displacer phase shifter. Appl Therm Eng 2022;205:117995. [\[CrossRef\]](#)
- [16] Guo Z, Zhu S. Regenerative effect of heat exchanger in pulse tube refrigerator. Int J Refrig 2020;118:114–120. [\[CrossRef\]](#)
- [17] Feng T, Tang Q, Liang ML, Wang N, Xun Y, Chen H, et al. A 598 g micro pulse tube cryocooler. Cryocoolers. 2021;21:157–161.
- [18] Zhang J, Zhao Y, Zhan J. CFD simulation of a micro pulse tube cryocooler operating over 100 Hz without reservoirs. Proceedings of 2022 IEEE 6th Information Technology and Mechatronics Engineering Conference (ITOEC); 2022. pp. 858–862. [\[CrossRef\]](#)
- [19] Li G, Feng T, Gao M, Liang M, Tang Q, Xun Y, et al. Design and optimization of a high frequency miniature pulse tube cryocooler. IOP Conf Ser Mater Sci Eng 2024;1301:012002. [\[CrossRef\]](#)
- [20] Min G, Li G, Feng T, Yang B, Quan J, Chen H, Cai J, Zheng M. The simulation and experiments of a high frequency single stage pulse tube cryocooler with two cooled thermal sinks. IOP Conf Ser Mater Sci Eng 2024;1301:012004. [\[CrossRef\]](#)
- [21] Wang N, Tang Q, Xun Y, Liang M, Zhao M, Chen H, et al. A lightweight high-capacity pulse tube cryocooler operating at 80 K. Cryogenics 2024;138:103800. [\[CrossRef\]](#)
- [22] Zhi X, He Y, Yang Z, Zhu H, Ying K, Qiu L. Study on the refrigeration performance of a miniature pulse tube cryocooler driven by a gas bearing compressor. Appl Therm Eng 2025;258:124508. [\[CrossRef\]](#)
- [23] Pfothenauer J, Shi J, Nellis GF. A parametric optimization of a single stage regenerator using REGEN 3.2. Cryocoolers 13 2005;463–470. [\[CrossRef\]](#)
- [24] Radebaugh R, O’Gallagher A, Gary J. Calculated regenerator performance at 4 K with helium-4 and helium-3. Adv Cryog Eng 2008;53:225–234. [\[CrossRef\]](#)
- [25] Wang B, Yao F, Zhou WJ, Gan ZH, Qiu LM. Study of a 35 K regenerator performance operating at high frequency. Cryocoolers 2011;16.
- [26] Thota S, Padmanabhan CS, Gurudath A, Amrit B, Basavaraj S, Dinesh K. Design of high frequency pulse tube cryocooler for onboard space applications. IOP Conf Ser Mater Sci Eng 2017;171:012081. [\[CrossRef\]](#)

- [27] Pfothenhauer JM, Wang RZ, Miller FK. Regenerator design optimization: Results from REGEN 3.3. *Cryogenics* 2019;97:77–84. [\[CrossRef\]](#)
- [28] Srinivasan KV, Manimaran A, Arulprakasajothi M, Pokale RD, Arolkar VA. Theoretical analysis on pressure drop across porous cryocooler regenerator in evaluating the optimum regenerator porosity. *Energy Sources Part A Recover Util Environ Eff* 2019;41:2045–2060. [\[CrossRef\]](#)
- [29] Srinivasan KV, Manimaran A, Arulprakasajothi M, Revanth M, Arolkar VA. Design and development of porous regenerator for Stirling cryocooler using additive manufacturing. *Therm Sci Eng Prog* 2019;11:195–203. [\[CrossRef\]](#)
- [30] Yadav CO, Ramana PV. Comparative study on performance of regenerator for miniature pulse tube cryocooler with metal matrix materials at ultra high frequencies. *Int J Air-Conditioning Refrig* 2021;29:2150033. [\[CrossRef\]](#)
- [31] Desai AB, Dutta R, Kant Verma S, Dewasi A, Agravat H, Gupta V, Mishra JS. Manifestation of improvement in regenerator performance of a low and high-frequency pulse tube cryocooler using layered pattern. *Therm Sci Eng Prog* 2023;45:102112. [\[CrossRef\]](#)
- [32] Chen X, Li S, Yu J, Yang S, Chen H. Rapid prediction of regenerator performance for regenerative cryogenics cryocooler based on convolutional neural network. *Int J Refrig* 2024;158:225–237. [\[CrossRef\]](#)
- [33] Gary J. REGEN 3.3: User Manual; 2008.
- [34] Kirkconnell C, Hon R, Perella M, Crittenden T, Ghiaasiaan S. Development of a miniature Stirling cryocooler for LWIR small satellite applications. *Proceedings of SPIE 10180, Tri-Technology Device Refrigeration (TTDR) II*, 5 May 2017, 1018002. [\[CrossRef\]](#)
- [35] Vanapalli S. High-frequency operation and miniaturization aspects of pulse-tube cryocoolers [dissertation]. Enschede: Universiteit Twente; 2008.
- [36] Garaway I, Zinn J, Bradley P, Veprik A, Radebaugh R. Development of a miniature 150 Hz pulse tube cryocooler. *Cryocoolers* 2009;15:105–113.